Examination of the Electrochemical Interface between Two Immiscible Electrolyte Solutions by Second Harmonic Generation

John C. Conboy and Geraldine L. Richmond*

Department of Chemistry, University of Oregon, Eugene, Oregon 97403

Received: September 10, 1996; In Final Form: December 3, 1996[⊗]

The potential-induced accumulation of electrolyte ions at the water/1,2-dichloroethane (DCE) electrochemical interface has been examined by total internal reflection second harmonic generation (TIR SHG). TIR SHG experiments provide the first direct optical measurements of the accumulation of the base electrolytes, tetraphenylarsonium (Ph_4As^+) and tetraphenylborate (Ph_4B^-), in the interfacial region between two immiscible electrolyte solutions (ITIES). The standard Galvani potential for ion transfer across the water/DCE interface for the tetrabutylammonium (TBA^+) is measured from the SHG data. Using the Ph_4As^+ ion as a reference, a value of 219 ± 5 mV is determined for TBA^+. In addition, optically determined potential-dependent concentration profiles for the Ph_4As^+ and Ph_4B^- ions are correlated with the modified Verwey−Niessen model for surface excess. Results suggest that less than 10% of the potential drop across the water/DCE interface occurs in the organic phase.

I. Introduction

The physical nature of the interface between two immiscible liquids continues to generate interest because of the central role that this interface plays in such processes as mass transport phenomena, charge transfer reactions, and extractions. The adsorption and transport of molecular and ionic species across a liquid/liquid phase boundary is dependent upon the structure of the interfacial region and the electrostatic and intermolecular forces therein. A detailed understanding of the structure and order of both solute and solvent molecules at the interface is therefore needed to better understand adsorption and transport properties at liquid/liquid interfaces. In recent years, progress has been made in the characterization of the interface between two immiscible electrolyte solutions (ITIES)[1] by employing such techniques as interfacial capacitance, electrocapillary studies, and potential of zero charge measurements.[2−4] The double-layer structure of these complex systems has been described by the modified Verwey−Niessen (MVN) model by means of Stern's modification to the Gouy−Chapman theory.[5,6]

Although the macroscopic parameters derived from experimental results are generally consistent with the MVN model, many unresolved issues remain. One question involves the presence or absence of an ion-free inner layer at the ITIES. Evidence for an ion-free inner layer has been sought by the determination of the potential of zero charge (pzc) for these systems. At the ITIES, the Galvani potential difference between the two phases ($\phi_w - \phi_o$) can be separated into contributions from the potential difference across the inner layer (ϕ_i) and the potential differences across the space charge regions in the organic (ϕ_2^o) and aqueous (ϕ_2^w) phases. The inner layer potential, ϕ_i, is the result of a dipolar contribution arising from solvent molecular orientation, while ϕ_2^o and ϕ_2^w are associated with the ionic charges present in the diffuse layer[3,4,7] (Figure 1). Gouy−Chapman (GC) theory predicts a rather high value for the potential drop across the inner layer[4] whereas differential capacitance and electrocapillary studies measure a relatively small value for water/1,2-dichloroethane (DCE) interface.[2,7] Several explanations have been offered to explain the difference in the observed values, including a random orientation of water molecules at the interface, a lack of any structure in the inner layer, or the absence of an ion-free inner layer altogether.[4,7,8] Such outstanding questions reveal a clear need for more direct measurements of the molecular properties of the ITIES.

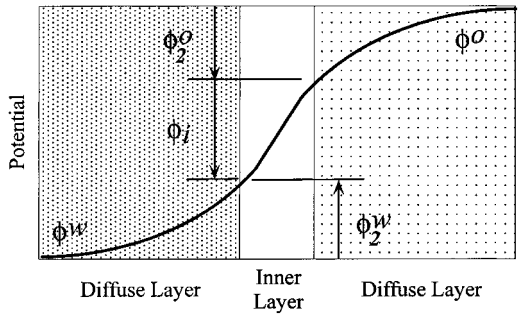

Figure 1. Schematic diagram of the modified Verwey−Niessen model of the ITIES.

A number of recent theoretical and experimental efforts have begun to shed light on the structure of the ITIES and the behavior of amphiphilic molecules residing at the oil/water interface. Molecular ordering of interfacial molecules in the water/DCE and water/DCE electrolyte systems has been the focus of recent molecular dynamics calculations.[9,10] The potential-induced adsorption and orientation of amphiphilic molecules at the water/DCE ITIES have been examined by resonant second harmonic generation (SHG) studies.[11,12] However, experimental studies that spectroscopically probe the microscopic properties of the native ITIES under potential control in the absence of probe ions have thus far been lacking. In order to address the fundamental questions about the ITIES, one needs direct spectroscopic measurements of ion accumulation and solvent composition of the double-layer region. The studies described in this and a previous paper[13] from this laboratory are directed specifically toward these goals.

The work described in this paper employs SHG, an inherently surface-specific technique. SHG has the ability to probe the interfacial region without contributions arising from the molecules in the bulk liquids which can complicate the interpretation. By applying an optical field of sufficient intensity at frequency ω, a second optical field is produced at twice the

* To whom correspondence should be addressed.
[⊗] Abstract published in *Advance ACS Abstracts,* January 15, 1997.

S1089-5647(96)02775-7 CCC: $14.00

frequency, 2ω. Analysis of the generated light at 2ω can reveal molecular information about the composition and ordering of the interface.[14] Under the electric-dipole approximation, SHG is not allowed in the bulk of centrosymmetric media such as liquids. At an interface, however, the distribution of material is discontinuous and the inversion symmetry is broken, lifting this restriction.[14] Because of this unique surface specificity, SHG has been exploited extensively to investigate a number of interfaces.[15−20]

In this study we have applied SHG to the enigmatic liquid/liquid electrochemical interface. The SHG experiments are performed in a total internal reflection (TIR) optical geometry. This technique, which has been developed in this laboratory for the investigation of liquid/liquid interfaces, results in an enhanced SHG response. The ITIES system, which is examined in detail here, is the water/1,2-dichloroethane electrolyte system. Experiments have been performed under both resonant and nonresonant conditions. These studies begin to address by spectroscopic means questions regarding the nature of the interface under potential control such as the accumulation of ionic species in the interfacial region and the presence or absence of an ion-free solvent layer. The SHG results are complemented by current−voltage measurements. These studies show that SHG is highly sensitive to the adsorption of aromatic ions such as tetraphenylarsonium and tetraphenylborate at the interface, and the results provide the first direct measurement of the relative concentration of these commonly used electrolyte ions at the interface as a function of potential.

II. Experimental Section

For the electrochemical and SHG experiments, the water was obtained from a NANOpureII water purification system with a measured resistivity of 17.8 Mohm cm. 1,2-Dichloroethane (99.8%), HPLC grade, was obtained from Sigma−Aldrich and used as received. The electrolytes for the aqueous and organic solutions, LiCl (99%) and tetrabutylammonium tetraphenylborate ($TBAPh_4B$; 99%), were purchased from Aldrich and used without any further purification. Tetraphenylarsonium tetraphenylborate (Ph_4AsPh_4B) was prepared by precipitation of tetraphenylarsonium chloride (Ph_4AsCl; 97%, Aldrich) and sodium tetraphenylborate ($NaPh_4B$; 99.5%, Aldrich) in methanol. The precipitate was filtered with hot methanol and then recrystallized from methylene chloride. The resulting crystals were then stored in a desiccator in the dark. Tetrabutylammonium chloride (TBACl; 98%, Aldrich) and Ph_4AsCl were used in the organic phase reference electrode.

The electrochemical measurements were performed with a Solartron 1286 four-electrode potentiostat. Measurements were performed with 1.0 mM aqueous solutions of LiCl and 1.0 mM Ph_4AsPh_4B or $TBAPh_4B$ in DCE. The aqueous and organic electrolyte solutions were equilibrated by shaking the solutions together prior to use. All solutions were filtered through a 0.5 μm Teflon filter to remove any particulates. Platinum wire coils were used as counter electrodes in the aqueous and organic phases and placed directly above and below the interface (Figure 2). The interfacial area employed was 1.75 cm^2. Ag/AgCl reference electrodes were used and housed in Luggin capillaries to reduce the *IR* drop due to the high solution resistance. The Luggin capillary in the organic phase housed the Ag/AgCl reference electrode in contact with an 10 mM aqueous solution of Ph_4AsCl or TBACl depending on the organic phase electrolyte used. The cell configuration is described by the scheme

$$\mathrm{Ag|AgCl|RCl(aq)|RPh_4B(DCE)||LiCl(aq)|Ag|AgCl} \quad (1)$$

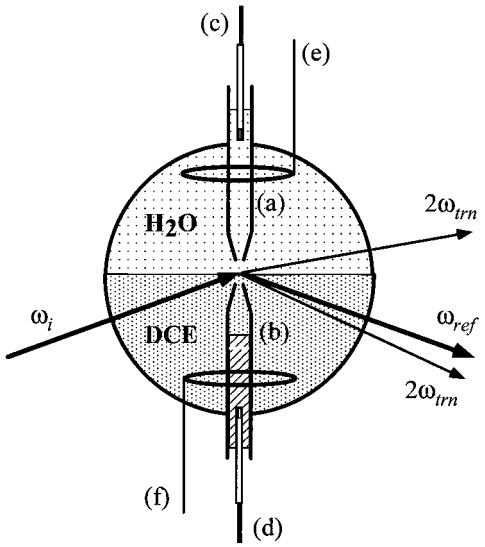

Figure 2. Diagram of the cylindrical quartz cell used for the electrochemical and SHG measurements. The cell contains an aqueous 1.0 mM LiCl solution in contact with a 1.0 mM solution of Ph_4AsPh_4B or $TBAPh_4B$ in DCE. The Luggin capillaries in the aqueous and organic phases are denoted by (a) and (b). A 10 mM aqueous solution of Ph_4AsCl or TBACl is used in (b) depending on the composition of the organic phase. Additional components of the cell are (c) and (d) the Ag/AgCl reference electrodes and (e) and (f) the platinum counter electrodes. The incident (ω_i) and reflected fundamental (ω_{ref}) beams are shown as well as the reflected ($2\omega_{ref}$) and transmitted ($2\omega_{trn}$) SH beams.

where R is the organic phase cation either Ph_4As^+ or TBA^+. The $RPh_4B(DCE)||LiCl(aq)$ interface is the one of interest. The applied potential to the cell, E_{app}, is defined using the convention previously established as the potential in the aqueous phase (w) minus the potential in the organic phase (o), $E_{app} = E_w - E_o$.[21,22]

The optical second harmonic measurements were performed in a cylindrical quartz cell which housed the reference (Luggins) and counter electrodes (Figure 2). Both the resonant and nonresonant optical SHG experiments were performed with a Quanta-Ray DCR11 Nd:YAG laser. Pulses of 10 ns duration and 2−5 mJ of incident energy at a repetition rate of 15 Hz were employed. The fundamental 1064 nm output of the Nd:YAG was used for the nonresonant experiments. For the resonant work the fundamental was frequency doubled in a KDP crystal to obtain 532 nm light. To achieve the angle of incident desired for total internal reflection, the incident laser beam was directed onto the interface through the 1,2-dichloroethane, the high index side of the interface. For the nonresonant experiments this was achieved at an angle of 71.5°. The SH light was collected in reflection at an angle of 70°. For the resonant investigations the incident angle was set to 67° from the surface normal with the generated SH light collected in transmission at an angle of 76°. The SH light was collected in transmission due to absorption of the SH light in the organic phase. Input polarization was controlled by a half-wave plate. The resulting SH light was polarization selected, filtered, and detected with a photomultiplier tube. Gated electronics were used for SH signal processing. For all the optical−electrochemical measurements the cell was cycled at a rate of 5 mV/s over the desired potential region. For the $LiCl/Ph_4AsPh_4B$ experiments the potential limits were 150−620 mV. For the $LiCl/TBAPh_4B$ experiments the limits were 200−520 mV. The potential was scanned continuously, and the SH intensity was recorded as a function of applied potential for a period of 30 min. The resulting SH signal was then averaged at 2 mV intervals over the entire potential range to obtain the resulting intensity data.

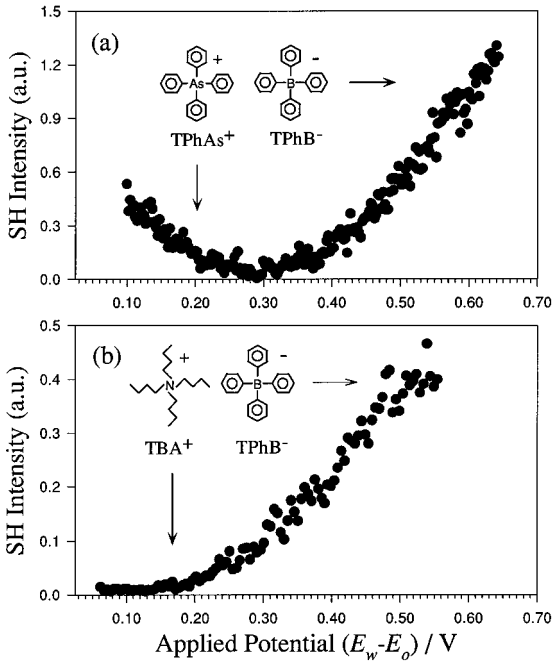

Figure 3. Nonresonant potential-dependent SH signal from the (a) 1.0 mM LiCl (H_2O)/1.0 mM Ph_4AsPh_4B (DCE) and (b) 1.0 mM LiCl (H_2O)/1.0 mM $TBAPh_4B$ (DCE) interfaces. The intensity data are for the m_{in},s_{out} polarization combination in both cases.

III. Results and Discussion

The nonresonant SH response from the LiCl/Ph_4AsPh_4B and LiCl/$TBAPh_4B$ systems under potential control is shown in Figure 3, a and b, respectively. The SH intensity clearly displays a potential dependence for the systems examined. This is the first observation of potential dependence in the nonresonant SH signal from the native. In previous studies by Higgins et al. and Naujok et al.,[11,12,23] no potential dependence was observed from the bare H_2O/DCE ITIES in the presence of $TBAPh_4B$. Instead, the potential-dependent adsorption of a surfactant, 4-((4-(dodecyloxy)azophenyl)benzoic acid, was measured with resonant SHG. These studies, however, cannot provide the same level of information about the double-layer structure of the native ITIES since the adsorption of an amphiphile to the H_2O/DCE interface significantly alters the double-layer structure. We attribute this difference to our enhanced sensitivity as a result of the TIR geometry. An increase in the SH intensity is observed when the system is biased positive of 300 mV for LiCl/Ph_4AsPh_4B and 200 mV for LiCl/$TBAPh_4B$. In addition, an increase in the SH intensity is observed for LiCl/Ph_4AsPh_4B at applied potentials below 300 mV.

Comparison of the data displayed in parts a and b of Figure 3 indicates that the SH intensity as a function of potential is dependent upon the organic phase electrolyte composition in two ways. First, the there is a positive potential shift in the SH intensity for Ph_4As^+ compared with TBA^+. An increase in the SH data is observed at ~200 mV for $TBAPh_4B$ whereas for Ph_4AsPh_4B the increase is not observed until a potential of greater than 300 mV is applied. Second, the SH data in Figure 3a show an increase in the SH intensity when biased below 300 mV for the Ph_4AsPh_4B electrolyte pair. Substitution of the aromatic Ph_4As^+ moiety for its alkyl analog TBA^+ results in the complete disappearance of any SH intensity at the same applied potentials for $TBAPh_4B$ (Figure 3b). By substituting the organic phase cation Ph_4As^+ for its less polarizable alkyl analog TBA^+, the SH intensity drops to levels comparable to what is observed from the neat water/1,2-dichloroethane interface.

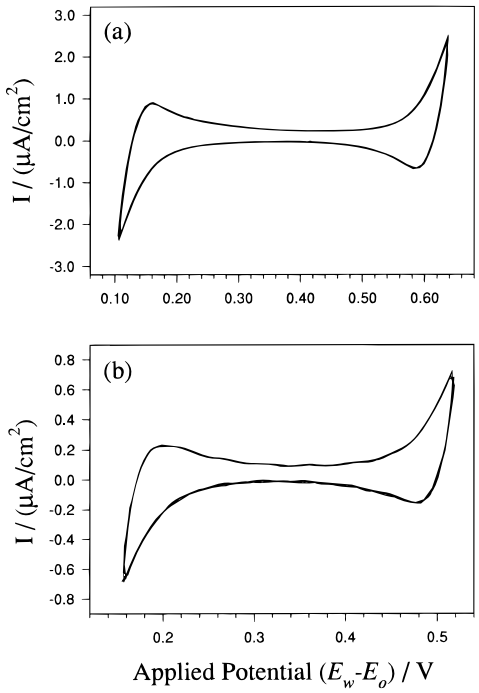

Figure 4. Cyclic voltammograms of the (a) 1.0 mM LiCl (H_2O)/1.0 mM Ph_4AsPh_4B (DCE) and (b) 1.0 mM LiCl (H_2O)/1.0 mM $TBAPh_4B$ (DCE) systems. The current was measured at a scan rate of 5 mV/s as a function of the potential difference between the aqueous and organic phases, $E_w - E_o$.

TABLE 1: Standard Gibbs Energies of Ion Transfer and the Corresponding Standard Galvani Potentials for the Water/1,2-Dichloroethane System[a]

	$\Delta_o^w G_i^o$/kJ mol^{-1}	$\Delta_o^w \varphi_i^o$/V
TBA^+	21.8	−0.225
Ph_4As^+	35.1	−0.364
Ph_4B^-	35.1	0.364
Cl^-	−46.4	−0.481
Li^+ [a]	−51.6	0.450

[a] The value for Li^+ was determined by extrapolating the data from the water/nitrobenzene interface.

The cyclic voltamograms (CVs) displaying the current versus voltage curves obtained from the two systems examined, LiCl/Ph_4AsPh_4B and LiCl/$TBAPh_4B$, are shown in Figure 4, a and b, respectively. These CVs display a capacitive character in the potential range 0.250−0.450 V for the Ph_4As^+ ion (Figure 4a) and 0.250−0.400 V for the TBA^+ (Figure 4b). A large current is measured for applied potentials greater than 500 mV and less than 200 mV in both systems. Using the conventions of previous authors,[21,22] the transfer of a positive charge from the aqueous to the organic phase is taken as the positive direction of current flow. The standard Gibbs energies and standard Galvani potentials of ion transport across the H_2O/DCE interface are given in Table 1.[24−27] The positive current flow in the CVs of Figure 4a,b is attributed to the transfer of Ph_4B^- from the organic to the aqueous phase, and the negative current is attributed to that of Ph_4As^+ (Figure 4a) or TBA^+ (Figure 4b). The current due to the transport of Cl^- and Li^+ is considered to be minimal due to the much higher transfer energies of these ions.[21,22]

Potential-Dependent SHG Response. To understand the potential dependence observed in the SH data in Figure 3a,b, possible contributing factors must be considered. The second harmonic intensity, $I^{2\omega}$, from the interface originates from the nonlinear polarization induced by the fundamental driving field at frequency ω.

$$I^{2\omega} \propto |P^{NL}|^2 \tag{2}$$

where $P^{NL} \propto \chi^{(2)}_{eff}:E(\omega)E(\omega)$ and $\chi^{(2)}_{eff}$ is the effective surface nonlinear susceptibility tensor and $E(\omega)$ the fundamental driving field. Since the liquid/liquid interface is rotationally invariant about the surface normal, there are only three nonvanishing independent elements of the surface nonlinear susceptibility tensor, $\chi^{(2)}_{eff}$, specifically χ^{eff}_{izi}, χ^{eff}_{zii}, and χ^{eff}_{izi} where $i = x, y$. The expressions for the SH intensity for the relevant polarization combinations are

$$I^{2\omega}_{Min},S_{out} = |f_y f_z \tilde{f}_y \chi^{eff}_{izi}|^2 \tag{3}$$

$$I^{2\omega}_{Sin},P_{out} = |f_y{}^2 \tilde{f}_z \chi^{eff}_{zii}|^2 \tag{4}$$

$$I^{2\omega}_{Pin},P_{out} = |f_x f_z \tilde{f}_x \chi^{eff}_{izi} + f_x{}^2 \tilde{f}_z \chi^{eff}_{zii} + f_z{}^2 \tilde{f}_z \chi^{eff}_{zzz}|^2 \tag{5}$$

where f and $\tilde{f}$ are the linear and nonlinear Fresnel factors, respectively, which are dependent upon the incident angle and the polarization of the fundamental light field.[28−32] The system coordinates are defined such that y is perpendicular to the plane of incidence and x and z lie in the plane. Polarizations are as follows: p-polarized, in the plane of incidence; s-polarized, perpendicular to the plane of incidence; and m-polarization, a mixture of both p and s components. The effective surface susceptibility, $\chi^{(2)}_{eff}$, can be expressed in terms of the molecular and electrostatic properties of the system. The former would arise from the molecular species at the interface, i.e., the accumulation of ionic species or solvent molecules. The electrostatic component would arise from the presence of the large electric field across the interface produced by the difference in electrochemical potentials between the two phases. With these factors taken into account, the effective surface nonlinear polarization can then be written as

$$\chi^{(2)}_{eff} = \chi^{(2)} + E_{dc}\chi^{(3)} \tag{6}$$

where $\chi^{(2)}$ is the second-order nonlinear susceptibility tensor, $\chi^{(3)}$ is the third-order nonlinear susceptibility tensor which possesses the same symmetry constraints as $\chi^{(2)}$, and E_{dc} is the local electric field strength at the interface. Both $\chi^{(2)}$ and $\chi^{(3)}$ are contingent upon the molecular composition and structure of the interface. The susceptibility tensors $\chi^{(2)}$ and $\chi^{(3)}$ contain contributions from the interfacial DCE and water molecules in addition to the molecular ions. For the solvent molecules the potential-dependent contribution would result from a change in molecular orientation as a result of the changing electric field or from the electric field itself resulting in an electric field induced second harmonic response (EFISH).[33] For the ions, the potential-dependent change in $\chi^{(2)}$ and $\chi^{(3)}$ would primarily come from accumulation of the ions in the diffuse layer.

In considering the change in $\chi^{(2)}$ with potential, the relative phase must be addressed. Examining the ionic species Ph_4As^+ and Ph_4B^- in which the central atom possesses a positive and a negative charge, respectively, the dipole along any carbon−arsenic versus a carbon−boron bond will have opposing dipoles. The net result would be that the absolute phase of $\chi^{(2)}$ for Ph_4As^+ should be 180° out of phase for that of Ph_4B^- with the consequence that $\chi^{(2)}$ will be opposite in sign for these two ions. In the case of multiple contributions one must also recognize that the elements of $\chi^{(2)}$ and $\chi^{(3)}$ and their associated Fresnel factors may be complex; thus, the possibility of interference between terms also exists.[34]

Referring back to the data in Figure 4, as the system is biased at potentials greater than 400 mV, the accumulation and transport of Ph_4B^- across the interface occur as determined electrochemically. A corresponding increase in the SH response is observed in Figure 3a,b in this potential region. However, when the interface is polarized at potentials less than 300 mV, an increase in the SH intensity is observed only for the Ph_4As^+ ion (Figure 3a) and not the TBA^+ ion (Figure 3b). Substitution of the aromatic Ph_4As^+ ion for the less polarizable TBA^+ ion results in the complete disappearance of any SH intensity even though the interfacial concentration of TBA^+ should be similar to that of Ph_4As^+ at these potentials. As noted above, this substitution also results in a drop in SH intensity at these more negative potentials that is comparable to that which is obtained from the neat water/1,2-dichloroethane interface. The cyclic voltammograms of Figure 4 and the electrochemical data in Table 1 support the idea that the potential-dependent SH response is arising from the migration of the aromatic and highly polarizable Ph_4As^+ and Ph_4B^- ions to the interfacial region. From this analysis the observed increase in the SH response in Figure 3a,b at positive potentials correlates with the positive current flow in the CVs of Figure 4a,b and is thus attributed to the accumulation of aromatic Ph_4B^- ion at the interface. Similarly, we attribute the increase in the SH intensity at potentials less than 300 mV in Figure 3a to the accumulation of Ph_4As^+ at the interface.

When considering the contribution due to $\chi^{(3)}$, it is important to remember that since this is a third-order processes, the magnitude of such an effect is 3−4 orders of magnitude smaller than contributions from $\chi^{(2)}$.[33] Thus, it is only when the magnitude of the electric field across the interface is relatively large that effects due to $\chi^{(3)}$ will contribute to any significant degree. If a $\chi^{(3)}$ effect was the dominate contribution to the SH response, the result would be a parabolic increase in the SH intensity as a function of applied potential as is seen for LiCl/Ph_4AsPh_4B. However, parabolic behavior is not observed in the SH data when the aromatic cation Ph_4As^+ is substituted for its alkyl analog TBA^+. This suggests that the potential-dependent SH response is dominated by a change in $\chi^{(2)}$ due to the accumulation of the organic phase ions at the interface. In agreement with this argument, previous resonant SH studies of surfactant adsorption at the water/DCE interface have shown that electric field effects were negligible.[11,12]

For the experiments described above which were conducted under nonresonant conditions, it is not possible to completely eliminate the possibility of contributions from $E_{dc}\chi^{(3)}$ in the observed potential dependence. Therefore, resonant SH experiments were also conducted on the $TBAPh_4B$/LiCl system to see whether any difference in the potential-dependent SH response could be observed when the SH response from the Ph_4B^- ion is significantly enhanced over other contributions. A resonant SH effect occurs when either the fundamental or the SH wavelengths are resonant with an optical transition in the material. Examination of the absorption spectra for the neat solvent, 1,2-dichloroethane (12.6 M), and a solution of $TBAPh_4B$ in acetonitrile (0.1 mM), Figure 5, shows that there is negligible absorption in the visible regions. It is only in the ultraviolet region that appreciable absorption occurs. The spectrum for 0.1 mM $TBAPh_4B$ in acetonitrile shows an absorption edge at 266 nm resulting from a $\pi \rightarrow \pi^*$ transition of the phenyl rings in the Ph_4B^- moiety. Since this transition is near the second harmonic wavelength of 266 nm when a fundamental wavelength of 532 nm is used, a resonant SH response from the aromatic Ph_4B^- ion can therefore be expected. The adsorption

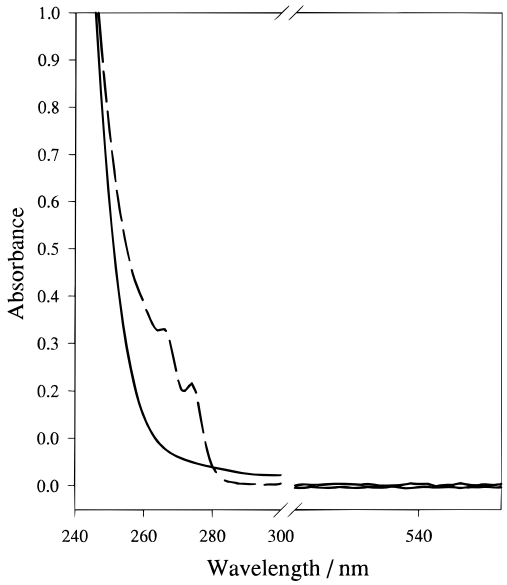

Figure 5. UV−vis absorption spectrum for DCE (—) and 0.1 mM $TBAPh_4B$ in acetonitrile (- - -).

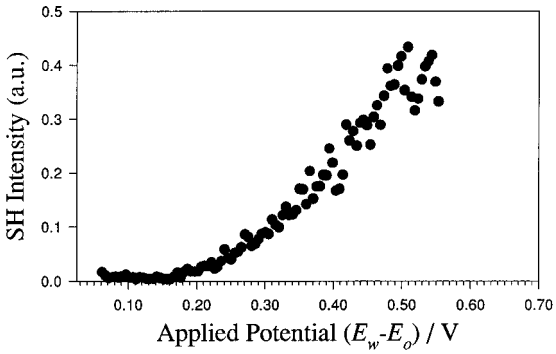

Figure 6. Resonant potential-dependent SH signal for the 1.0 mM LiCl (H_2O)/1.0 mM $TBAPh_4B$ (DCE) interface. The intensity data are for the s_{in},p_{out} polarization combination.

of the solvent and electrolyte near 266 nm also precludes the possibility of using the reflected component of the SHG light.

Due to dispersion, a transmitted as well as a reflected SH field is produced by the nonlinear polarization induced at the interface, even when the fundamental is under total internal reflection.[29,32] The frequency-dependent refractive indices of the liquids results in the SH at 2ω achieving TIR at an incidence angle larger than the critical angle of the fundamental at ω. The enhancement obtained under TIR for the reflected SH field has been shown to hold for the transmitted SH field.[35] This optical geometry is critical to measuring the resonant SH response from the electrochemical interface or ITIES composed of an aqueous phase of LiCl and an organic phase of $TBAPh_4B$ in DCE. Both the DCE and $TBAPh_4B$ absorb at 266 nm, as seen in their respective absorption spectra shown in Figure 5. Measurement of the SH response therefore cannot be performed in reflection due to the high absorptivity in the organic phase. However, due to the symmetric nature of the induced SH field, the SH light propagated in transmission can be used.

Figure 6 shows the results obtained from the resonant experiment. An increase in the SH response is observed for potentials greater than 300 mV with the SH intensity leveling off to background levels in the lower potential region. As with the nonresonant studies, the observed potential dependence is attributed solely to the Ph_4B^- ion accumulation at positive potentials. Comparison of the nonresonant results of Figure 3b with the those shown in Figure 6 indicates that the potential dependence of the SH response from these systems is identical regardless of whether the experiment is conducted under resonant or nonresonant conditions. In both the resonant and nonresonant studies, the absence of any increase in the SHG signal intensity at potentials less than 100 mV in the presence of the relatively nonpolarizable TBA^+ ion suggests that neither potential-induced solvent orientation nor EFISH processes are insignificant factors. This conclusion further supports the notion that the potential-dependent SH response is due entirely to the accumulation of Ph_4B^- and Ph_4As^+ ions at the interface for the nonresonant experiments.

SHG Minima and the PZC. One important goal of these experiments has been to explore whether the potential of zero charge can be determined optically for such ITIES systems. In the past there has been considerable controversy in the determination of the pzc for these systems. Referring to the CVs of Figure 4, the potential applied to the interface is referenced to the organic phase cation, TBA^+ or Ph_4As^+. The Luggin capillary housing the Ag/AgCl reference electrode (left-hand side of eq 1), which is in contact with the aqueous RCl (R = TBA^+ or Ph_4As^+) solution, effectively functions as an ion selective electrode reversible to the R^+ ion. The RCl(aq)|RPh_4B (DCE) interface, which occurs just inside the Luggin capillary, is nonpolarizable with the potential difference across the interface being determined by the TBA^+ or Ph_4As^+ cations.[21,22] The Galvani potential difference, $\Delta\varphi_o^w$, between the aqueous and organic phases can be obtained from the applied potential, E_{app}, from eq 2[36]

$$\Delta\varphi_o^w = E_{app} + \Delta_o^{w'}\varphi_{R^+}^o + (RT/F)\ln(\gamma_{R^+}^o c^o\alpha/\gamma_{R^+}^{w'}c^{w'}) \quad (7)$$

where $\Delta_o^w\varphi_{R+}^o$ is the standard Galvani potential difference for R^+ (Ph_4As^+, TBA^+), a is the degree of dissociation of RPh_4B in 1,2-dichloroethane, γ is the mean activity coefficient, and c^o and $c^{w\prime}$ are the concentration of RPh_4B in the organic and reference electrode solutions, respectively. The mean activity coefficient γ and the degree of dissociation α were determined by the equations[36]

$$\log\gamma_+ = -A\sqrt{c^o\alpha}/(1 + Ba\sqrt{c^o\alpha}) \quad (8)$$

$$K_a = (1-\alpha)/\gamma_+^2 c^o\alpha^2 \quad (9)$$

where A and Ba are parameters of Debye−Huckel theory and K_a is the association constant. For Ph_4AsPh_4B and $TBAPh_4B$ the values of Semac et al. were used (A = 10.19 $M^{-1/2}$ and Ba = 6.07 $M^{-1/2}$).[36] The association constant, K_a, used for Ph_4AsPh_4B and $TBAPh_4B$ in 1,2-dichloroethane was 1.175×10^3 and 6.00×10^2, respectively.[37] The potential of zero charge ($\Delta\varphi_o^w = 0$) determined from the data in Table 1 and eqs 8 and 9 is calculated to be at an applied potential, E_{app}, of 440 mV for Ph_4As^+ and 305 mV for TBA^+.

Examination of the potential-dependent SH data of Figure 3a,b shows a positive potential shift in the SH intensity data for Ph_4AsPh_4B compared to $TBAPh_4B$. The increase in the SH intensity at potentials greater than 300 mV has been attributed to the accumulation of the Ph_4B^- ion for both systems. The potential shift in the SH intensity data is the result of the shift in the pzc for these two systems due to the variation of the organic phase cation. The pzc for Ph_4As^+ resides 135 mV above the pzc for TBA^+. As a result, the accumulation of Ph_4B^- occurs at greater applied potentials for the LiCl/Ph_4AsPh_4B ITIES than for the corresponding LiCl/$TBAPh_4B$ system. This is verified by the fact that the potential difference in the SH intensity data between LiCl/Ph_4AsPh_4B and LiCl/$TBAPh_4B$ is

130 mV, very close to the difference between the pzc for these two systems.

With similar thermodynamic properties for the Ph_4B^- and Ph_4As^+ ions, one would expect the minimum in the potential-dependent SH data of Figure 3a at 0.290 V to correspond to the pzc for this systems. At the pzc the interface is charge neutral with the concentration of Ph_4B^- and Ph_4As^+ being equal. In comparing the observed minimum in the SH intensity data of Figure 3a for Ph_4AsPh_4B with the calculated pzc value of 440 mV for Ph_4AsPh_4B in DCE, there appears to be a potential shift in the optical data in reference to the electrochemical state of the interface of approximately 160 mV. Similar potential shifts have been observed in the SH response from the metal/electrolyte interface.[17,38−41] For such interfaces the SH response is dominated by the electric field present at the interface. As mentioned earlier in this paper, the observed potential dependence for the ITIES has been concluded to be the result of the accumulation of the aromatic ions at the interface. Contributions due to third-order processes, $\chi^{(3)}$, were determined to be minimal realtive to $\chi^{(2)}$, where $\chi^{(2)}$ is dependent upon the accumulation of the aromatic ions at the interface. However, similar to the metal/electrolyte interface, the SH response from the ITIES can be modeled by considering a constant susceptibility term, $\chi^{\text{eff}}_{(l-l)}$, and a term involving the variation of the concentration of electrolyte species Ph_4As^+ and Ph_4B^-, $\chi^{\text{eff}}(i)$. An expression for the SH intensity can then be written for the system which will have the form

$$I^{2\omega}_{\text{ITIES}}(\varphi) \propto |F\chi^{\text{eff}}_{(l-l)} + F\chi^{\text{eff}}_{(\text{i})}(\varphi)|^2 \tag{10}$$

where F's are the Fresnel factors and φ is the rational potential. The term $\vec{\chi}^{\text{eff}}_{(i)}$ can be considered the sum of the contributions from both the Ph_4As^+ and Ph_4B^- ions:

$$\chi^{\text{eff}}_{(\text{i})} \propto \sum_i N_i \chi^{\text{eff}}_i \tag{11}$$

where N is the interfacial concentration of the ion. The elements of $\chi^{\text{eff}}_{(i)}$ are also complex quantities that change sign depending on the charge of the ion. Equation 10 then describes a parabola, assuming a linear dependence of the concentration of Ph_4As^+ and Ph_4B^- on the potential φ, with the minima shifted by the quantity $F\chi^{\text{eff}}_{(l-l)}$.

In considering the physical factors that could be contributing to the component $\chi^{\text{eff}}_{(l-l)}$ several possibilities exist. This static term could result from H_2O and DCE, which exist in excess at the interface and the concentration of which varies little as the potential is changed. Another possibility is an ion-free inner layer residing between the two space charge regions in the aqueous and organic phases, the composition of which would be invariant upon alteration of the applied potential. Electrocapillary and capacitance data support the presence of an ion-free inner layer on the aqueous side of the interface with the inner layer thickness on the order of a monolayer of water.[22]

Support for the conclusion that a static $\chi^{\text{eff}}_{(l-l)}$ term is contributing and results in a shift of the parabolic minimum in the SHG data from the pzc comes from polarization studies. Different polarization combinations of the fundamental and SH light will result in a variation of the Fresnel factors. Variation of the Fresnel factors will result in a shift in the intensity minima as a function of applied potential by scaling the magnitude of $\chi^{\text{eff}}_{(l-l)}$, eq 10. This can be clearly demonstrated here for the LiCl/Ph_4AsPh_4B ITIES. The SH intensity as a function of potential for the $Ph_4AsThPhB$/LiCl system under nonresonant conditions for the m_{in},s_{out} and s_{in},p_{out} polarization combinations is shown in Figure 8, a and b, respectively. Comparison of the

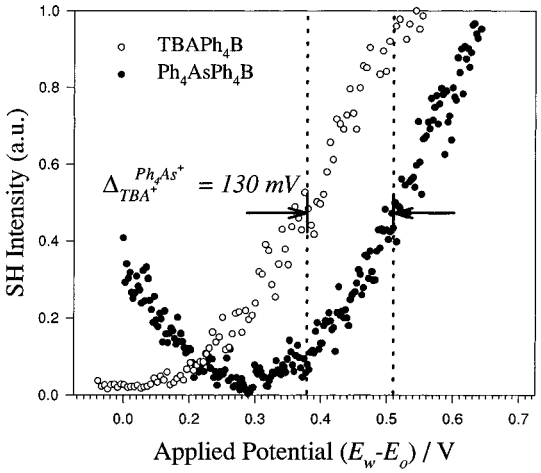

Figure 7. Nonresonant potential-dependent SH signal from the (●) 1.0 mM LiCl (H_2O)/1.0 mM Ph_4AsPh_4B (DCE) and (○) 1.0 mM LiCl (H_2O)/1.0 mM $TBAPh_4B$ (DCE) interfaces. The intensity data are for the s_{in},p_{out} polarization combination in both cases. A potential shift of 105 mV in the SH data is observed upon substitution of TBA^+ for Ph_4As^+

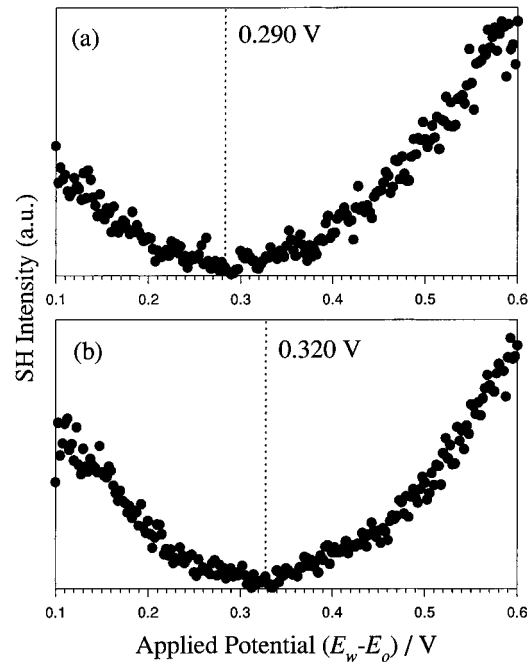

Figure 8. SH intensity data displaying the anisotropic shift in the SHG minima for the Ph_4AsPh_4B system for (a) *mixed* p_{in},s_{out} and (b) s_{in},p_{out} polarization combinations.

intensity data for the two polarization combination clearly shows a shift in the intensity minima as the polarization is changed.

Determination of Galvani Potentials of Ion Transfer. It is possible to use the optical data to retrieve relevant thermodynamic information about the standard Gibbs energies of ion transfer and the corresponding standard Galvani potentials of the organic phase ions. For example, the determination of the standard Galvani potential of ion transfer for a given ion can be obtained from the SH data. In particular, the standard Galvani potential of the TBA^+ ion at −225 mV has been questioned by some authors.[7] The determination of the actual value is extremely important since conclusions regarding the double-layer structure of the ITIES obtained from the evaluation of the pzc for the these systems have been based on this value.[7,42]

By comparing the potential-dependent SH data for the TBA^+ and Ph_4As^+ systems, we can address this issue. The standard Gibbs energies of ion transport and standard Galvani potentials

for a given ion cannot be measured directly. Values are determined by an extrathermodynamic approach and as a result are always related to the corresponding quantity for another ion. The most widely accepted standard has been the Ph_4AsPh_4B pair since it is assumed that both the cation and anion have the same standard Gibbs energy for ion transport between any arbitrary pair of solvents.[43] In this same fashion the SH data can be used to determine the standard potential difference for the TBA^+ ion. If the assumption is made that the standard potential difference for the Ph_4As^+ is -364 mV, we can use this value to determine the value for TBA^+ much in the same way standard potential differences or the standard Gibbs energies of individual ions are determined electrochemically. Figure 7 shows the SH data for both the Ph_4AsPh_4B and $TBAPh_4B$ systems. The rise in the SH intensity at potential greater than 300 mV was determined to be the result of the Ph_4B^- ion accumulation at the interface. There is a potential difference between the two systems of 130 mV, which is due to the substitution of the Ph_4As^+ ion for TBA^+ resulting in a shift in the pzc for these systems, eq 7. Using the standard potentials of -0.364 and -0.225 V for the Ph_4As^+ and TBA^+ ions, the potential of zero charge for the two systems was determined to be 440 and 305 mV, respectively. The potential difference between the two systems would then be 135 mV, very close to the 130 mV which is obtained from the optical measurements. The standard potential for the TBA^+ ion can be determined using eq 2. Using the potential difference of 130 mV gives a value of -219 ± 5 mV for the standard Galvani potential of the TBA^+ ion, very close to the literature value of -225 mV.

Relative Concentration of Ions at the Interface. The SH response also provides a basis for determining the relative concentration of ions at the interface as a function of the applied potential, assuming contributions from electric field effects are negligible as suggested previously. The SH intensity has been shown to be dependent upon the $TPhAs^+$ and $TPhB^-$ ions at the interface. Optical interference between the response from the two ions Ph_4As^+ and Ph_4B^- is also minimal since such interference would result in slightly different intensity profiles for the Ph_4B^- ion for $LiCl/Ph_4AsPh_4B$ and $LiCl/TBAPh_4B$, which is not observed. Thus, the minima in the SH data are the result of the depletion of organic phase ionic species from the interface.

The SH intensity has been shown to be dependent upon the concentration of Ph_4As^+ and Ph_4B^- ions at the interface. Consequently, the potential-dependent SH data can be used to make an optical measurement of the relative interfacial concentrations of these ionic species by taking the square root of the SHG signal intensity. The square root of the SHG signal intensity, as displayed in Figure 9, is proportional to the surface concentration of the Ph_4As^+ and Ph_4B^- ions as seen in eq 11. Also shown is the concentration profile of Ph_4As^+ and Ph_4B^- obtained from the modified Verwey−Niessen model (MVN). In the MVN model the potential drop across the interface is divided into three contributions:

$$\Delta\varphi_o^w = \varphi_i + \varphi_2^o - \varphi_2^w \tag{12}$$

where φ_2^o and φ_2^w are the potentials dropped in the organic and aqueous phases space charge regions, respectively, and φ_i is the potential difference across the inner solvent layer[5] (Figure 1). The concentration profile was obtained using the equations for the surface excess, Γ_i^o ($i = Ph_4As^+$ or Ph_4B^-), given by[7]

$$\Gamma_i^o = (A^o/F)[\exp(\mp F\varphi'/2RT) - 1] \tag{13}$$

with

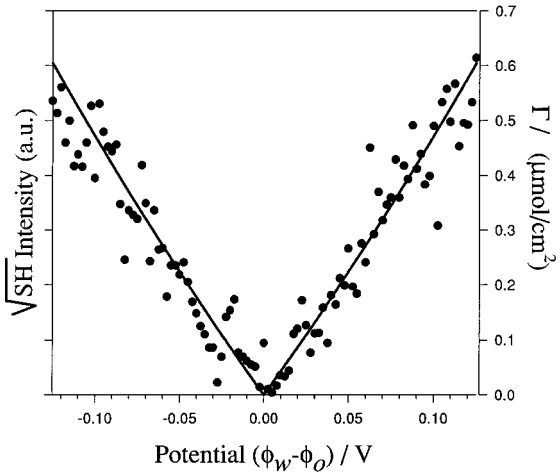

Figure 9. $\sqrt{I_{SHG}}$ for LiCl (H_2O)/Ph_4AsPh_4B (DCE), s_{in},p_{out} polarization (○), and the calculated surface excess from the MVN model (—).

$$A^o = (2RT\epsilon^o\epsilon_0 c^o)^{1/2} \tag{14}$$

where ϵ^o and ϵ_0 are the permittivity of DCE and a vacuum, respectively, and c^o is the bulk concentration of Ph_4AsPh_4B, in this case 1.0 mM. The SH data were fit to the surface excess of eq 14 using a single fitting factor f, which represents a fraction of the total potential difference across the interface, $\varphi' = f\Delta\varphi_o^w$. Excellent agreement between the optical data and the surface excess profile is obtained when less than 10% of the total potential difference is dropped in the organic phase space charge region.

The fact that the optical data suggest that the majority of the potential is dropped in the aqueous phase is consistent with the much higher dielectric constant of water (78.25) over that of DCE (10.2). This observation is also consistent with the fact that the organic phase ions are not completely dissociated. In addition, it has also been suggested that a portion of the potential is also dropped within the inner layer itself, a claim supported by electrocapillary and capacitance measurements.[2−4] In the work of Kakiuchi and Senda[21,22] in which surface excess charge and surface ion excess were determined for the TBA^+ and Ph_4B^- ions at the ideally polarizable water/nitrobenzene interface, a layer of water molecules thicker than a monolayer was needed in order to obtain agreement between the calculated surface excess and the experimental data. The technique described here may not be capable of optically measuring all the species present in the diffuse layer. If true, then only a fraction of the ions responsible for the potential drop would be measured. The method here, however, is capable of establishing a lower limit to the total potential drop within the organic phase space charge region.

IV. Conclusions

The technique of TIR SHG has been applied to the investigation of the interface between two immiscible electrolyte solutions. By employing TIR SHG, the first potential-dependent SH response for the native ITIES composed of an aqueous solution of 1.0 mM LiCl and 1.0 mM Ph_4AsPh_4B and $TBAPh_4B$ in DCE has been obtained. Several important conclusions are drawn for the behavior of the SH response under potential control. For both resonant and nonresonant experiments the potential-dependent SHG response is attributed to the induced accumulation of the aromatic Ph_4As^+ and Ph_4B^- ions at the interface. These results are substantiated by examination of the electrochemical data for these systems, in particular the standard Gibbs energies of ion transport. Comparison of experiments

performed under both resonant and nonresonant conditions shows contributions from electric field induced SHG (EFISH) effects to be minimal as well are contributions from solvent orientation.

With the SH response being dominated by the accumulation of the aromatic ionic species Ph_4As^+ and Ph_4B^- in the interfacial region, the minimum in the SH response for the Ph_4AsPh_4B/LiCl system is found to be shifted form the electrochemically derived pzc by 160 mV. This potential shift is interpreted in terms of static component to the nonlinear susceptibility, possibly arising from the presence of a layer of solvent molecules residing between the two phases which is essentially free of any ionic species and is invariant with applied potential. By comparing the potential-dependent SH data for the TBA^+ and Ph_4As^+ systems, the standard Galvani potential for the TBA^+ is measured. Using the standard potential of -0.364 V for the Ph_4As^+, the value of 219 ± 5 mV is determined for the TBA^+ ion from the potential-dependent SH data.

TIR SHG measurements are shown to be a complement to electrocapillary and capacitance measurements in the determination of electrolyte surface excess. Optically determined potential-dependent concentration profiles obtained from the SH data for the Ph_4As^+ and Ph_4B^- ions have been correlated with the modified Verwey−Niessen model for surface excess. TIR SHG complements measurements of the electrolyte surface excess and can function as an optical means of measuring the relative concentration of electrolytic species responsible for the potential drop in the diffuse layer. The results obtained form this analysis suggest that less than 10% of the potential drop across the water/DCE interface occurs in the organic phase.

The successful demonstration of the use of TIR SHG at the ITIES greatly expands the capability to study ion adsorption and transport at liquid/liquid interfaces. The use of TIR SHG at liquid/liquid junctions can provide a means by which the properties and processes of this broad range of interfaces can be studied in detail. Electrochemical methods have historically be used to address the fundamental nature of the ITIES. With the use of TIR SHG and related techniques the investigation of these buried interfaces is now accessible by optical means.

Acknowledgment. The authors gratefully acknowledge the National Science Foundation (NSF CHE-9416856) for financial support of this work. Additional thanks also goes to Ted Hinke for construction of the electrochemical/optical cell.

References and Notes

(1) Karzarinov, V. E. *The Interface Structure and Electrochemical Processes at the Boundary between Two Immiscible Liquids*; Springer-Verlag: Berlin, 1897.
(2) Girault, H. H. J.; Schiffrin, D. J. *J. Electroanal. Chem.* **1984**, *161*, 415.
(3) Koczorowski, Z.; Paleska, I.; Kotowski, J. *J. Electroanal. Chem.* **1987**, *225*, 65.
(4) Senda, M.; Kakiuchi, T.; Osahai, T. *Electrochim. Acta* **1991**, *36*, 253.
(5) Verwey, E. J. W.; Niessen, K. F. *Philos. Mag.* **1939**, *28*, 435.
(6) Gavach, C.; Seta, P.; d'Epenoux, B. J. *J. Electroanal. Chem. Interfacial Electrochem.* **1977**, *83*, 225.
(7) Samec, Z. *Chem. Rev.* **1988**, *88*, 617.
(8) Girault, H. H. *Electrochim. Acta* **1987**, *32*, 383.
(9) Benjamin, I. *J. Chem. Phys.* **1992**, *97*, 1432.
(10) Benjamin, I. *Science* **1993**, *261*, 1158.
(11) Higgins, D. A.; Naujok, R. R.; Corn, R. M. *Chem. Phys. Lett.* **1993**, *213*, 485.
(12) Higgins, D. A.; Corn, R. M. *J. Phys. Chem.* **1993**, *97*, 489.
(13) Conboy, J. C.; Richmond, G. L. *Electrochim. Acta* **1995**, *40*, 2881.
(14) Shen, Y. R. *The Principles of Nonlinear Optics*; Wiley: New York, 1984.
(15) Shen, Y. R. *Nature* **1989**, *337*, 519.
(16) Shen, Y. R. *Annu. Rev. Phys. Chem.* **1989**, *40*, 327.
(17) Richmond, G. L.; Robinson, J. M.; Shannon, V. L. *Prog. Surf. Sci.* **1988**, *28*, 1.
(18) Heinz, T. F. In *Surface Nonlinear Electromagnetic Phenomena*; Ponath, H., Stegmam, G. I., Eds.; Elsevier: Amsterdam, 1992.
(19) Eisenthal, K. B. *Annu. Rev. Phys. Chem.* **1992**, *43*, 627.
(20) Corn, R. M. *Anal. Chem.* **1991**, *63*, A285.
(21) Kakiuchi, T.; Senda, M. *Bull. Chem. Soc. Jpn.* **1983**, *56*, 1322.
(22) Kakiuchi, T.; Senda, M. *Bull. Chem. Soc. Jpn.* **1983**, *56*, 1753.
(23) Naujok, R. R.; Higgins, D. A.; Hanken, D. G.; Corn, R. M. *J. Chem. Soc., Faraday Trans.* **1995**, *91*, 1411.
(24) Rais, J. *Collect. Czech. Chem. Commun.* **1971**, *36*, 3253.
(25) Rais, J. *J. Inorg. Nucl. Chem.* **1976**, *38*, 1376.
(26) Geblewicz, G.; Koczorowski, Z. *Colloid Interface Sci.* **1983**, *158*, 37.
(27) Koczorowski, Z.; Geblewicz, G. *Colloid Interface Sci.* **1983**, *152*, 55.
(28) Guyot-Sionnest, P.; Shen, Y. R.; Heinz, T. F. *Appl. Phys. B* **1987**, *42*, 237.
(29) Bloembergen, N.; Pershan, P. S. *Phys. Rev.* **1962**, *128*, 606.
(30) Bloembergen, N. *Opt. Acta* **1966**, *13*, 311.
(31) Bloembergen, N.; Simmon, H. J.; Lee, C. H. *Phys. Rev.* **1969**, *181*, 1261.
(32) Dick, B.; Gierulski, A.; Marowsky, G. *Appl. Phys. B* **1987**, *42*, 237.
(33) Butcher, P. N.; Cotter, D. *The Elements of Nonlinear Optics*; Cambridge University Press: New York, 1990.
(34) Tadjeddine, A.; Guyot-Sionnest, P. *J. Phys. Chem.* **1990**, *94*, 5195.
(35) Conboy, J. C.; Richmond, G. L. *J. Phys. Chem.* **1994**, *98*, 9688.
(36) Samec, Z.; Marecek, V.; Holub, K.; Racinshy, S.; Hajkova, P. *J. Electroanal. Chem.* **1987**, *225*, 65.
(37) Abraham, M. H.; Danil de Namor, A. F. *J. Chem. Soc., Faraday Trans.* **1975**, *72*, 955.
(38) Richmond, G. L. *Chem. Phys. Lett.* **1984**, *110*, 571.
(39) Rojhantalab, H. M.; Richmond, G. L. *J. Phys. Chem.* **1989**, *93*, 3269.
(40) Guyot-Sionnest, P.; Tajeddine, A. *Chem. Phys. Lett.* **1990**, *5*, 172.
(41) Corn, R. M.; Romagnoli, M.; Levenson, M. D.; Philpott, R. *Chem. Phys. Lett.* **1984**, *106*, 30.
(42) Samec, Z.; Marecek, V.; Homolka, D. *Faraday Discuss. Chem. Soc.* **1984**, *77*, 277.
(43) Park, A. J. *Electrochim. Acta* **1976**, *21*, 671.